HHS Public Access

Author manuscript

Brain Res. Author manuscript; available in PMC 2016 March 14.

Published in final edited form as:

Brain Res. 2007 August 8; 1162: 98–112. doi:10.1016/j.brainres.2007.05.018.

Alterations in striatal dopamine catabolism precede loss of substantia nigra neurons in a mouse model of Juvenile Neuronal Ceroid Lipofuscinosis

Jill M. Weimer[1], **Jared W. Benedict**[1,2], **Yasser M. Elshatory**[1], **Douglas W. Short**[1,3], **Denia Ramirez-Montealegre**[1], **Deborah A. Ryan**[1], **Noreen A. Alexander**[5,6], **Howard J. Federoff**[1,4], **Jonathan D. Cooper**[5,6], and **David A. Pearce**[1,3,4,*]

[1]Center for Aging and Developmental Biology, University of Rochester School of Medicine and Dentistry, Rochester, New York 14642

[2]Department of Biochemistry and Biophysics, University of Rochester School of Medicine and Dentistry, Rochester, New York 14642

[3]Department of Environmental Medicine, University of Rochester School of Medicine and Dentistry, Rochester, New York 14642

[4]Department of Neurology, University of Rochester School of Medicine and Dentistry, Rochester, New York 14642

[5]Pediatric Storage Disorders Laboratory, King's College London, Institute of Psychiatry, De Crespigny Park, London, SE5 8AF, UK

[6]Department of Neuroscience, Centre for the Cellular Basis of Behaviour, King's College London, Institute of Psychiatry, De Crespigny Park, London, SE5 8AF, UK

Abstract

Batten disease, or juvenile neuronal ceroid lipofuscinosis (JNCL), results from mutations in the *CLN3* gene. This disorder presents clinically around the age of five years with visual deficits progressing to include seizures, cognitive impairment, motor deterioration, hallucinations, and premature death by the third to forth decade of life. The motor deficits include coordination and gait abnormalities, myoclonic jerks, inability to initiate movements, and spasticity. Previous work from our laboratory has identified an early reduction in catechol-O-methyltransferase (COMT), an enzyme responsible for the efficient degradation of dopamine. Alterations in the kinetics of dopamine metabolism could cause the accumulation of undegraded or unsequestered dopamine leading to the formation of toxic dopamine intermediates. We report an imbalance in the catabolism of dopamine in three month *Cln3*$^{-/-}$ mice persisting through nine months of age that may be causal to oxidative damage within the striatum at nine months of age. Combined with the

*To whom reprint requests should be addressed at: David A. Pearce, University of Rochester School of Medicine and Dentistry, Center for Aging and Developmental Biology, Box 645, Rochester, New York 14642, (585) 273-1514, (585) 276-1972 Fax, david_pearce@urmc.rochester.edu.

previously reported inflammatory changes and loss of post-synaptic D1α receptors, this could facilitate cell loss in striatal projection regions and underlie a general locomotion deficit that becomes apparent at twelve months of age in *Cln3*$^{-/-}$ mice. This study provides evidence for early changes in the kinetics of COMT in the *Cln3*$^{-/-}$ mouse striatum, affecting the turnover of dopamine, likely leading to neuron loss and motor deficits. These data provide novel insights into the basis of motor deficits in JNCL and how alterations in dopamine catabolism may result in oxidative damage and localized neuronal loss in this disorder.

Keywords

Batten disease; Catechol-O-methyltransferase; *CLN3*; dopamine; oxidative stress

1. Introduction

Juvenile Neuronal Ceroid Lipofuscinosis (JNCL) is an autosomal recessive neurodegenerative disorder with an average age of onset around five years with patients typically not surviving past their third decade of life. This disease, resulting mutation of the *CLN3* gene, manifests with visual deficits but progresses to include seizures, motor problems, cognitive impairment, and, in some cases, hallucinations and schizophreniclike behavior. The extrapyramidal motor deficits associated with the disease include stereotypic cog-wheel rigidity, balance impairment, hypokinesia, flexed posture, and shuffling gait that typically render patients immobile by their mid-teens (Hofman et al., 1999).

Imaging studies in JNCL patients have shown dysfunction in the striatum as measured by a reduction in dopamine transporter (DAT) levels and [^{18}F] fluorodopa uptake, an analog of dopamine (Ruottinen et al., 1997; Aberg et al., 2000). Once released into the synaptic cleft, dopamine activates either the D1 or D2 class of receptors. PET studies of JNCL patients showed a reduction in the striatal D1, but not D2 receptors (Rinne et al., 2002). In this study, we have investigated these basal ganglia deficits in *Cln3* knockout mice (*Cln3*$^{-/-}$), a mouse model of Batten disease. Although NCL mouse models have shown many similar pathological characteristic as patients (Mitchison et al., 1999; Seigel et al., 2002; Sappington et al., 2003; Pontikis et al., 2004; Pontikis et al., 2005; Kielar et al., 2007), neuroanatomical analysis of the *Cln3*$^{-/-}$mice has failed to reveal any regional volumetric changes of the striatum, although detailed analysis of target cell loss in this area has not been performed (Pontikis et al., 2004). Interestingly, in the *Cln3*$^{-/-}$ mice, as well as other NCL models, there is a marked increase in the levels of both reactive astrocytes and microglia within this compartment, indicative of cellular damage (Pontikis et al., 2004; Pontikis et al., 2005; Kielar et al., 2007). Interestingly, gene expression studies of the *Cln3*$^{-/-}$ mouse brain have uncovered a marked decrease in the expression of catechol-O-methyl transferase (COMT) (Elshatory et al., 2003). This is a key enzyme involved in the degradation of catecholamines within the striatum, as well as other brain regions, calling into question the integrity of the metabolism and function of this neurotransmitter family in the *Cln3*$^{-/-}$ mouse. Although limited behavioral analysis of these mice has unmasked cerebellar related motor deficits (Kovacs et al., 2006), no analysis of basal ganglia specific motor changes has yet been performed.

In this study, we demonstrate a reduction in both the protein and activity levels of COMT in *Cln3*$^{-/-}$ mice by three months of age which results in an alteration in the degradation of catecholamines. Specifically, we show a decrease in the levels and catabolism of dopamine. We reasoned that a diminution of dopamine catabolism would lead to elevation in reactive oxidative forms of dopamine, particularly within the non-vesicular compartment, that could increase oxidative damage within the striatum. Recent attempts to elucidate the events leading up to cell loss and microglial activation in the *Cln3*$^{-/-}$ mice have demonstrated elevated oxidative burden in different anatomical compartments, often with activated microglial located immediately adjacent to neurons reactive for potent antioxidant markers (Benedict et al., 2007). Elevated oxidative stress within the striatum could result from or trigger the previously reported inflammatory response (Pontikis et al., 2004), subsequently leading to restricted cellular changes, including the post-synaptic receptor down regulation reported in JNCL (Rinne et al., 2002). Indeed, we saw a marked increase in oxidized proteins and the down regulation of D1α receptors in the *Cln3*$^{-/-}$ striatum by nine months of age, paralleling the increase in glial activation. In exploring whether this alteration within the basal ganglia culminate in cell loss in afferent or efferent striatal targets, we demonstrated a loss of parvalbumin positive substantia nigra pars reticulata neurons at nine months. Therefore, this suggests that an early decrease in COMT activity in the *Cln3*$^{-/-}$ mice leads to dramatic changes in catabolism of dopamine, ultimately affecting striatal circuitry, including oxidative damage and progressive loss of nigral neurons. This cell loss provides a plausible explanation for the motor deficits we report in *Cln3*$^{-/-}$ mice and provides a likely mechanism for the extrapyramidal dysfunction seen in JNCL patients.

2. Results

2.1 Disruption in key enzyme involved in catecholamine catabolism in Cln3$^{-/-}$ *mice*

The *Cln3*$^{-/-}$ mouse model for Batten disease has a substantial decrease in the levels of catechol-O-methyl transferase (*Comt*) mRNA in the brain (Elshatory et al., 2003). This enzyme, along with monoamine oxidase, MAO, facilitates the degradation of dopamine both within the striatum and other portions of the nervous system (Fig 1A). Degradation of norepinephrine requires two additional enzymes, aldehyde reductase and aldehyde dehydrogenase (Fig 1B). Mining of several published microarray data sets performed on the *Cln3*$^{-/-}$ mice showed a selective downregulation in the expression of *Comt* but none of the other enzymes involved in catecholamine catabolism were altered (Fig 1A & 1B) (Brooks et al., 2003; Elshatory et al., 2003). Normal synthesis of catecholamines is achieved through conversion of tyrosine to DOPA, dopamine, norepinephrine, and epinephrine, sequentially. Disruption in the initial synthesis of catecholamines could impact downstream regulation of these proteins, as well as enzymes involved in their turn-over. Enzymes involved in the production of catecholamines, specifically tyrosine hydroxylase, DOPA decarboxylase, dopamine β-hydroxylase, and norephinephrine N-methyltransferase (*Pnmt*) were also included in the previously conducted microarray studies. Of these enzymes, none were altered in the *Cln3*$^{-/-}$ mice except a slight, yet significant, decrease in the level of *Pnmt*, suggesting disruption in the enzyme involved in conversion of norepinephrine to epinephrine [less than 1.5 fold change, p=0.049, 10-week whole brain microarray (Brooks et

al., 2003)] (Fig 1C). Therefore, we chose to further explore COMT as a putative enzymes involved in the pathogenesis of Batten disease.

To establish that this decrease in *Comt* mRNA levels translated to alterations in protein levels, we performed immunoblotting analysis for COMT on proteins from microdissected cortex and striatum samples. COMT is found in the brain in two forms, as a predominant, high affinity membrane bound (MB-COMT) isoform located primarily in the rough-ER, and in a low affinity, soluble isoform (S-COMT) found throughout the cytosol and nucleus (Salminen et al., 1990; Lundstrom et al., 1991; Malherbe et al., 1992; Winqvist et al., 1992). COMT has been shown to be most prevalent within the prefrontal cortex, however, biochemical and immunohistological studies have demonstrated this enzyme to be present in nearly all mammalian tissues (Guldberg and Marsden, 1975). Comparison of COMT protein levels in wild-type and *Cln3*$^{-/-}$ mice in various brain regions revealed isoform-specific, brain region, and age-dependent differences.

In frontal cortex, while COMT protein levels were not different between wild-type and *Cln3*$^{-/-}$ mice at three months of age, by nine months of age, *Cln3*$^{-/-}$ cortex showed lower levels of MB-COMT (Fig. 2A). The most apparent changes in COMT were found in the striatum, where there were decreased COMT protein levels at both three and nine months of age, with the S-COMT being significantly lower at three months and the MB-COMT by nine months (Fig. 2B). Thus, MB-COMT protein levels were decreased in the cortex and striatum of nine month *Cln3*$^{-/-}$ mice, while S-COMT protein levels decreased in the striatum only at three months of age.

To establish whether alterations in the ratio of soluble to membrane COMT levels affect the activity of this enzyme, we assayed the function of both forms of this protein by the *O*-methylation of dihydroxybenzoic acid in protein extracts. Within the cerebral cortex, the activity level of both forms of COMT paralleled the decreases in protein levels at three months of age, although by nine months of age there was not a significant change in activity (Fig. 2A). Within the striatum, early reductions in the expression of COMT followed closely with a reduction in the activity of the enzyme which was maintained at nine months of age, demonstrating a substantial, prolonged impairment in the levels and function of this enzyme (Fig. 2B).

In summary, within the striatum, there is a global reduction in both the low affinity soluble and high affinity membrane bound form of the enzyme occurring as early as three months of age which persists at nine months of age. Deficits in this enzyme are not restricted to the striatum, with both the frontal cortex and cerebellum (data not shown) showing impairment in COMT levels and function. The low affinity, soluble form is predominately expressed within astrocytes of the brain, where as the MB-COMT is primarily found in neurons (Rivett et al., 1983a, b). Although neuroanatomical analysis has failed to reveal any volumetric decrease in the striatum of *Cln3*$^{-/-}$ mice, by five months of age there is an elevation in both reactive astrocytes and microglia within this compartment, indicative of on-going cellular damage and targeted cellular stress within the striatum (Pontikis et al., 2004).

2.2 Disruption in dopamine catabolism in Cln3$^{-/-}$ mice

To explore whether decreased activity of COMT within the *Cln3*$^{-/-}$ mice influenced turnover of catecholamines, we examined the levels of dopamine and its metabolites using HPLC-EC in cortical and striatal samples. At both three and nine months, there was a significant decrease in the level of dopamine in both the cerebral cortex and at three months within the striatum (Fig. 3A-B). These findings demonstrate an overall decrease in the levels of dopamine in *Cln3*$^{-/-}$ mice. Several mechanisms could account for this decrease in dopamine levels which is apparent by three months of age. One possibility is that there is an alteration in the metabolism of dopamine. Alternatively, decreases in dopamine could be the result of an increase in dopamine oxidation. Once oxidized, the dopamine may form covalent adducts on proteins, which in turn would cause a shift from the normal dopamine peak making the levels of dopamine appear artificially low.

A decrease in the activity of enzymes that degrade catecholamines, such as COMT, could alter the catabolism of dopamine. This process occurs by two alterative pathways, either degradation via COMT, leading to the formation of homovanillic acid (HVA) via an homovanillyl-aldehyde intermediate, or by monoamine oxidase B, also leading to the formation of HVA, but via a 3,4-dihydroxyphenylacetic acid (DOPAC) intermediate (Kandel et al., 2000). Therefore, by comparing levels of dopamine, and two of these major metabolites, DOPAC and HVA, the effectiveness of COMT versus MAO-B catabolism of dopamine may be determined. The levels of HVA and DOPAC in three and nine month old *Cln3*$^{-/-}$ and 129/SvJ wild-type mice in cortex and midbrain were measured by HPLC-EC. This analysis revealed global disruption in the levels of the DOPAC metabolite. In the cerebral cortex there was a ∼ 10 fold decrease in the levels of DOPAC at three months of age (Fig. 3A), whereas there were significant decrease in the levels DOPAC within the striatum, with a greater than 9 fold reduction in the level of this metabolite at three months and a ∼5 fold reduction at nine months of age (Fig. 3B). These findings reveal a significant alteration in the catabolism of dopamine in both brain regions. One would speculate that, in order to maintain a comparable level of HVA with a decrease in COMT there would have to be a substantial increase in the levels of DOPAC. Instead there was a marked decrease in the levels DOPAC, suggesting that the machinery involved in dopamine catabolism is slowing in response to the decreased levels of dopamine. Additionally, this decrease in catabolism could increase the amount of time the residual dopamine is free within the synapse. Therefore, the frontal cortex and striatum [as well as similar observations noted in the cerebellum (data not shown)] are profoundly affected in *Cln3*$^{-/-}$ mice.

2.3 Alteration in dopamine catabolism within the striatum leads to an increase in oxidative stress and loss of neurons in the Cln3$^{-/-}$ mice

Alterations in COMT activity can potentially have confounding effects on the striatum. The presence of elevated levels of undegraded dopamine within the synaptic compartment could lead to the appearance of toxic, reactive oxidative derivatives of dopamine. These toxic intermediates have been shown to promote oxidative damage in several neurodegenerative disease, including Parkinson and Alzheimer's disease (Dalle-Donne et al., 2003a; Glaser et al., 2005; Hsu et al., 2005). To determine whether there is elevated oxidative stress within the striatum of *Cln3*$^{-/-}$ mice, we measured the levels of protein carbonyls within the striatum

and cortex. Derivatization of carbonyl groups on amino acid side chains with 2,4-dinitrophenylhydrazine (DNPH) leads to the formation of a stable product, 2,4-dinitrophenyl (DNP) hydrozone which can be detected using an antibody to DNP (Dalle-Donne et al., 2003b). At three months of age, there was no change between wild-type and *Cln3*$^{-/-}$ mice in the level of DNP, but at nine months of age there was a significant increase in the level of carbonyls within the striatum of *Cln3*$^{-/-}$mice (Fig. 4A). No changes were noted in the cerebral cortex again suggesting that these changes are restricted to the striatum (Fig. 4A). Appearance of oxidative damage within the striatum lags behind alterations in COMT activity, as well as, in the appearance of microglial activation, suggesting that oxidative stress due to carbonylation occurs only in the later stages of disease pathogenesis.

Microglia activation, oxidative damage, and cellular stress within the striatum could have multiple effects, not only on cells within the striatum itself, but also cells which project to and from this region. It has been previously demonstrated in the *Cln3*$^{-/-}$mouse that by as late as 15 months of age there is no overall atrophy of the striatum, suggesting gross preservation of this brain region (Pontikis et al., 2004). This same study showed an increase in the activation of both microglia and astrocytes within the striatum by five months of age, suggesting that an ongoing cellular insult occurs within this region of the brain. These changes in oxidative damage and glia activation could have direct effects upon cell populations which project to and from the striatum. Cells within the substantia nigra pars compacta (SNpc) receive modulatory projections from the striatum. Additionally, cells in the substantia nigra pars reticulata (SNpr) receive efferent connections from cells of the striatum and project to the thalamus. We first explored whether there were regional volume changes within either of these connection regions by performing Cavalieri estimates of volume at 6 months of age, an intermediate time point between when we first noted changes in COMT levels and elevation in oxidative damage within the striatum. Indeed, we saw a decrease in the volume of the SNpr of the *Cln3*$^{-/-}$mouse at six months of age (Fig. 4B). To determine whether regional volume changes were the result of either cell loss or a decrease in individual cell size, we performed optical fractionator cell counts. We used parvalbumin (PV) stained sections, to visualize the GABAergic neurons of the pars reticulata, or tyrosine hydroxylase (TH) stained sections, to visualize the dopaminergic neurons of the pars compacta. Although there was a substantial decrease in the volume of the SNpr at six months of age, there was not a significant loss of PV positive cells within this region until nine months of age (Fig 4C). By this time point, there was a near 35% reduction in the number of cells within SNpr of the *Cln3*$^{-/-}$ mice. In contrast, the TH positive cells of the SNpc remained preserved even at the later time points (Fig. 4D). The TH positive cells of neighboring ventral tegmental area (VTA) also appeared preserved (data not shown). Nucleator estimates of neuronal volume detected no change in the size of the remaining neurons within either region at six months of age (data not shown).

2.4 Degeneration in motor skills in the Cln3$^{-/-}$ mouse

To explore whether these cellular and molecular perturbation of the basal ganglia circuitry results in defects in motor skills, we evaluated locomotor behavior at three, nine, and twelve months of age to determine whether there was a compromise in general motor activity by evaluating total motor output in distance and time. Although no differences in these

parameters were observed between genotypes at three or nine months of age, by twelve months of age there was an overt impairment in locomotor activity (Fig. 5). At this later time point, *Cln3*$^{-/-}$ mice showed a ∼3 fold reduction in the total distance traveled and a ∼2 fold reduction in the total amount of time spent ambulating during the 30 minute test session (Fig. 5E-F). These impairments were spread evenly across the 30 minute trial period with no detectable differences within individual 50 msec time intervals. This demonstrates that these differences are not the result of slowness in initiating movements at the onset of the trial or a tiring of the animal.

2.5 Compensation for decreased COMT activity

Within the striatum, inhibition of COMT activity and alteration in dopamine levels could lead to changes within the microenvironment of the synapse. Because undegraded dopamine can auto-oxidize and lead to the formation of chemically reactive intermediates which are capable of promoting oxidative damage, cells within the striatum might up-regulate other proteins, shifting toward an alternative pathway for sequestering or degrading this catecholamine.

Although COMT has been associated with post-synaptic medium spiny neurons within the striatum, this enzyme predominantly resides within astrocytes juxtaposed to the synapse. Astrocytes do not express a dopamine specific transporter; therefore, movement of dopamine into these cells is facilitated by the norepinephrine transporter (NET). Although different isoforms of NET are expressed in the brain (Porzgen et al., 1995), there were no changes in the protein levels of the predominant 69kD transporter at either three or nine months of age in the striatum or the cerebral cortex of the *Cln3*$^{-/-}$ mice (Fig S1). The dopamine transporter (DAT) is a plasma membrane transporter expressed at presynaptic terminals and facilitates the reuptake of dopamine into nigral projection neurons. Due to the potential for an increase in undegraded dopamine within the striatum, we investigated whether these afferent terminals altered the levels of DAT in an effort to sequester dopamine into the presynaptic terminals. Western blot analysis showed no difference in the level of the 75 kD DAT protein in the *Cln3*$^{-/-}$ mouse (Fig S1). These data suggest that this potential alteration in dopamine catabolism does not result in the compensatory up regulation of catecholamine specific transporters. The activity of NET and DAT is regulated by the intracellular signaling events and the subsequent internalization of the transporter complex. Therefore, we can not rule out the possibility that NET or DAT's activity is being down-regulated by removal of the protein from the cell surface (Torres et al., 2003; Holton et al., 2005).

Once sequestered within the presynaptic terminals via the DAT transporter, dopamine can either be repackaged into synaptic vesicles by the vesicular monoamine transporter (VMAT) for re-release or degraded by the monoamine oxidase enzyme, MAO-B. Examination of levels of both VMAT and MAO-B revealed that neither was altered in an immunoblot assay, suggesting that there are not compensatory changes in the level of the proteins involved in the intracellular handling of dopamine in the presynaptic nerve terminals of the substantia nigra pars compacta (data not shown). However, the finding that there is a decrease in the

dopamine metabolite DOPAC (Fig. 3), which is specific to the MAO pathway of degradation, does indicate compromise in some aspect of this catabolic pathway.

Alteration in the levels of synaptic dopamine levels could affect receptor expression on post-synaptic neurons of the striatum. The D1α and D2 receptors are the post-synaptic dopaminergic receptors and establish the direct and indirect pathway between the striatum and output nuclei of the basal ganglia (Kandel et al., 2000). Patients with Batten disease have a down-regulation in the expression of D1α receptor of the medium spiny striatal neurons (Rinne et al., 2002). To address whether a similar decrease in receptor levels occurs in the *Cln3*$^{-/-}$ mice, western blot analysis was performed on cortical and striatal samples at three and nine months of age. A significant decrease in D1α receptor levels was noted by nine months of age within the striatum, though no difference was seen at the earlier time point (Fig. 6). Additionally, there was no change in D1α receptor levels within the cortex of the *Cln3*$^{-/-}$ mice. These findings confirm that post-synaptic changes that occur within the *Cln3*$^{-/-}$ mouse striatum resemble those seen in JNCL patients. Moreover, these data suggest that although alterations in the levels of COMT protein and activity occur in the *Cln3*$^{-/-}$ mice as early as three months of age, the effect on post-synaptic proteins is not seen until a number of months later.

3. Discussion

Mechanisms by which JNCL patients develop motor deficits during the mid- to late-stages of the disease are poorly understood and exploration of these changes in human patients has been limited to imaging studies. Connections in the basal ganglia nuclei are thought to fine tune motor signals relayed via the cortex and thalamus and alterations within any aspect of this circuitry alters movements. In this study, using a genetic mouse model of JNCL, we demonstrate alterations in MB-COMT and S-COMT protein and activity levels which are most apparent in the striatum of the *Cln3*$^{-/-}$ mice. The alterations in dopamine metabolism that we report are summarized in Figure 7. COMT catalyzes the transfer of a methyl group from *S*-adenosyl-ι-methionine to one of the hydroxyls of a catechol, leading to catecholamine inactivation (Axelrod and Tomchick, 1958). In addition, a shift in the ratio of membrane to soluble form of COMT, as seen in this study, alters the kinetics of dopamine metabolism (Guldberg and Marsden, 1975). Over time, this is likely to lead to an accumulation of undegraded, unsequestered dopamine which auto-oxidizes, initiating an increase in oxidative damage as we demonstrated by an increased carbonyl burden. Eventually, this cellular stress could progress to the down regulation of the D1α receptor that we see that is similar to that seen in the striatum of JNCL patients (Rinne et al., 2002).

In addition to early changes in COMT levels, these findings reveal a substantial overall decrease in the levels of dopamine in the *Cln3*$^{-/-}$ mice. There is no apparent disruption in the enzymes involved in catecholamine synthesis. The decrease in COMT could result in excess dopamine that could auto-oxidize within the synaptic compartment. HPLC-EC methods used here would be inefficient at detecting these modified forms of dopamine, which are unstable and that quickly adduct with other proteins. Regardless of the precise mechanism involved, there is a significant decrease in functional dopamine within the brain of *Cln3*$^{-/-}$ mice as well as a decrease in dopamine catabolism, as measured by decreases in DOPAC levels.

Alterations in COMT could precipitate blunted dopamine catabolism, or alternatively, a decrease in the global levels of dopamine could lead to a decrease in the production of enzymes essential for degradation. Although the present data are insufficient to determine which of these cellular events occurs first and further studies will be required to determine the exact time course of these early events, we do demonstrate that oxidative damage does not occur until later ages in the striatum of the *Cln3*$^{-/-}$ mice. Although sustained oxidative stress within this cellular compartment could exacerbate glial activation and ultimately lead to cell death within the striatum, close examination of the timing of these events is suggestive that oxidative damage is only occurring secondarily to other earlier molecular and pathological events occurring within the striatum. Nevertheless, the changes we report offer a plausible explanation for precipitating the loss of neurons in striatal projection regions and, ultimately in motor deficits that are measurable in *Cln3*$^{-/-}$ mice. The initial motor analysis presented here provides evidence for a degenerative change in locomotor activity dependant on a progressive loss of cells within the substantia nigra paralleling the late-stage onset of motor changes seen in JNCL patients. Recently, we have reported a defect in motor coordination by as early as two months of age in *Cln3*$^{-/-}$ mice (Kovacs et al., 2006). Although these deficits appear to be cerebellar specific and distinguishable from the late onset general locomotor impairment reported here, we cannot rule out that coordination deficits may be confounding overall locomotor activity, warranting a sophisticated assessment of these motor impediments.

Prior to this study, the only reported changes within the striatum of JNCL patients have come from imaging studies and observations of motor deficits in patients. A year long study where JNCL patients were treated with L-DOPA, the precursor of dopamine, revealed an initial response with a significant improvement on a Unified Parkinson Disease Rating Scale (UPDRS) although these patients did not respond as well to treatment as idiopathic Parkinson patients (Aberg et al., 2001). Concomitant administration of COMT inhibitors with L-DOPA, or the genetic predisposition to express COMT with a diminished activity, has been suggested to increase the benefits of L-DOPA (Tai and Wu, 2002). As such, the decreased levels of COMT evident in *Cln3*$^{-/-}$mice, and presumably JNCL patients, might create an environment more conducive to L-DOPA treatment. The improvement observed in JNCL patients treated with L-DOPA was not permanent though and after approximately twelve months UPDRS scores returned to pretreatment levels. Interestingly, a case study of late infantile NCL (LINCL) showed a decrease in cerebrospinal fluid levels of HVA and HVA:DOPAC ratios, suggesting a similar deficit in dopamine turnover exist in patients with LINCL, as well as, providing a useful model for measurement and detection of altered dopamine metabolites in patients (Barisic et al., 2003). Not unlike the JNCL patients, subsequent treatment with L-DOPA proved ineffective in treatment. Therefore, a more comprehensive assessment of the molecular changes affecting dopamine metabolism and COMT activity in JNCL patients would be prudent in lieu of continued L-DOPA therapy.

In addition to affecting the central nervous system (CNS), decreases in the level of COMT could have confounding affects on other systems by impeding subsequent degradation of catecholamines, including norepinephrine and epinephrine, both which rely on dopamine as a precursor. As these catecholamines regulate cardiovascular function, in tandem with a

depression in COMT activity, disruption in their metabolism could lead to aberrant stimulation of the heart. Aside from the reported pathology in the CNS, the only other system to be affected in JCNL patients is the cardiovascular system. Abnormalities become apparent in the later stages of the disease and can include bradycardia and poor blood flow and exploration of whether alterations in catecholamine levels affect the cardiovascular system in JNCL patients is necessary (Hofman et al., 1999). The mechanism by which loss of *CLN3* would result in changes in the level of COMT and catecholamines remains elusive, as does the manner in which this loss targets oxidative damage to the striatum while sparing the cortex. We demonstrate a decrease in the number of GABAergic neurons in the SNpr but observed no change in number of dopaminergic neurons in the SNpc. As the only dopamine producing cells of the basal ganglia, the observation of a decrease in dopamine within the striatum would suggest that cells of the SNpc, although not reduced in number, may have significant functional impairment. Previous analysis of neuroanatomical changes within the striatum have focused on changes in structural volume, which could reflex not only changes in cell number but also alterations in the cell volume, invasion of activated glial cells, or compensatory changes in the associated neuropil. This study provides a framework for a more detailed assessment of neuronal populations within the striatum, suggesting that cells projecting to the SNpr may be selectively targeted. Based on the previous findings of decreased D1α receptor expression in JNCL, we investigated whether the expression of this receptor were changed in *Cln3*$^{-/-}$ mice. It should be reiterated that, in addition to D1α, medium spiny neurons, as well as presynaptic terminals within the striatum, also express the D2 class of receptors. This receptor is known to be autoregulated by the levels of dopamine within the synaptic cleft. Therefore, changes in this class of receptors can not be excluded and changes could further contribute to the pathology reported here in *Cln3*$^{-/-}$ mice.

Disruption in dopamine function could contribute to both the motor deficits as well as the Schizophrenic like behaviors associated with Batten disease. Indeed, polymorphisms within COMT have been reported to decrease the levels of enzyme within the brain (Weinshilboum and Raymond, 1977; Boudikova et al., 1990) and have been associated with Schizophrenia, motor impairments, and cognitive decline, (Fan et al., 2005; Galderisi et al., 2005; Horowitz et al., 2005). As JNCL progresses, hallucinations and Schizophrenic-like behavior becomes common. Recently, Disc-1, a gene believed to be involved in cortical development and linked to Schizophrenia, has been shown to be naturally mutated in the 129S6/SvEv genetic background (Koike et al., 2006), the same strain of mice as the *Cln3*$^{-/-}$ mice. This would suggest that while some of our findings may be pertinent to Schizophrenic-like symptoms in Batten disease, that these mice are not an appropriate model as this aspect of Batten disease.

The function of CLN3 protein remains unknown, however, recent studies have suggested a role for CLN3 in cellular transport (Fossale et al., 2004; Luiro et al., 2004; Weimer et al., 2005). Therefore, loss of CLN3 may affect not only the intracellular transport of various cargos, but the communication between neuronal populations. A recent study reported that lymphoblasts from patients with JNCL had decreased levels of the amino acid arginine, as well as altered transport of this molecule across the lysosomal membrane (Ramirez-Montealegre and Pearce, 2005). Although a common link between dopamine and arginine metabolism is not known, there are certain reports of catecholamines influencing nitric oxide

biosynthesis from arginine through transport into cells of this amino acid (Lin et al., 2005). As studies of *Cln3*$^{-/-}$ mice unveil vulnerable cell populations, comparative studies between the relative cellular expression of *CLN3* and disease progression could provide further insights into the function of CLN3, and its influence on the metabolism of molecules such as arginine and dopamine. In this study we provide novel evidence for oxidative damage within the striatum leading to selective degeneration of cells within the efferent nigral region, providing potential insight into JNCL progression. By narrowing the cause of this neuronal loss to an enzymatic alteration within the striatum, this study has provided valuable information on the pathogenesis of JNCL and could provide new therapeutic targets aimed at alleviating exptrapyramidal motor deficits associated with the disease and preventing further nigral degeneration.

4. Experimental Procedures

4.1 Locomotor activity and motor function

Automated open field locomotor activity chambers equipped with infrared photobeams (Med Associates, St. Albans, Vermont) were used to quantify locomotor activity. Mice were initially habituated to the locomotor activity chambers in two 30-min sessions occurring on consecutive days. Animals were habituated at the same time each day and housed in a room with a 12 hour light-dark cycle between testing. On the third day, locomotor testing was performed identical to the pre-testing habituation for 30 minutes. Photobeam breaks were recorded every 50 msec for 30 min for horizontal, vertical and ambulatory movements. Separate groups of mice were tested at three, nine, and twelve months of age and results of locomotor activity are reported as the means of total distance each animal traveled or the amount of time spent moving within the 30 minute test interval. To further discern differences in distance and time traveled, we compared between genotype at each 50 msec recorded interval for distance or time. Data were analyzed by two-way ANOVA and presented as mean ± SEM; asterisks indicate significance compared with control at $P \leq 0.05$ (Bonferroni's post-hoc t-test).

4.2 Tissue preparation and Immunoblotting

129/SvJ and homozygous *Cln3*$^{-/-}$ mice on a 129/SvJ background were used for this study. All procedures were carried out in accordance with NIH guidelines and the University of Rochester Animal Care and Use Committee Guidelines with all animals housed under identical conditions. Cortex and striatum samples were microdissected from three and nine month old *Cln3*$^{-/-}$ and wild type (129/SvJ/SVJ) mice (n=6/test group). Samples were prepared solely from male mice to avoid the complication of sex differential expression of COMT. Tissue was flash-frozen immediately upon collection, and then homogenized on ice in approximately four volumes of ice-cold 50mM sodium phosphate buffer (0.5mM DTT, pH 7.5) using a motor-driven homogenizer. Protease inhibitors (Sigma, St. Louis, MO) and 2 × solubilization buffer (50 mM sodium phosphate buffer, pH 7.5, 0.5 mM DTT, 0.2% SDS) were added. Protein concentration was determined on aliquots from each of the tissue homogenates using a Lowry protein assay (BioRad Inc., Hercules, CA). SDS PAGE (10-13%) and immunoblotting was performed using standard techniques (as outlined in Elshatory, et al, 2003). Antibodies used for immunoblotting included anti-β-Actin (Sigma,

St. Louis MO), anti-COMT (Transduction Labs, Lexington, KY), anti-DAT, anti-D1α (Chemicon, Temecula, CA), and anti-MAO-B (Santa Cruz Biotechnologies, Santa Cruz, CA). Immunoblots were exposed to film for various lengths of time and scanned for densitometry using AlphaImager v5.5 (Imgen Technologies, Alexandria, VA) and the mean pixel density of each protein of interest was normalized to the mean pixel density of β-Actin.

4.3 MB-COMT and S-COMT Activity Assays

Cortex and striatum samples were microdissected from three and nine month old *Cln3*$^{-/-}$ and wild type (129/SvJ/SVJ) mice (*n*=3/test group). Following homogenization, 500μl of homogenate was ultracentrifuged in a Beckman Optima TL ultracentrifuge using a TLA 100.2 rotor for 30 minutes at 2°C (48,000RPM or 100,000×G). The supernatant, enriched in S-COMT, was placed in a fresh tube, and the pellet, enriched in MB-COMT, was resuspended in 500μl of ice-cold 50mM sodium phosphate buffer (0.5mM DTT, pH 7.5) and placed in a fresh tube. Prior to performing the COMT assay, an aliquot of the soluble and pellet fractions were used to estimate protein concentration and for western blot analysis to confirm proper separation of the MB- and S-COMT isoforms. The COMT assay used here is a modified version of those described previously (Reenila et al., 1995; Reenila et al., 1997; Ellingson et al., 1999; Pihlavisto and Reenila, 2002). Reaction samples contained 180μl of tissue (from either the S- or the MB-COMT-enriched fractions) in a total reaction volume of 500μl. $MgCl_2$ was added to a final concentration of 5.5mM, and the COMT co-substrate S-adenosylmethionine was added to a final concentration of 2mM. The COMT substrate used, dihydroxybenzoic acid (DHBAc), was added to a final concentration of 0.2mM to start the reactions. Samples were incubated at 37°C for 60 minutes, upon which time reactions were terminated with the addition of 100μl of 2M $HClO_4$. Reaction blanks contained all of the above components with the exception of tissue extract. Another reaction control contained all reaction components above in addition to $CaCl_2$ (2.5mM), which, at this concentration, inhibits COMT activity by about fifty percent. The reaction product peak for vanillic acid was detected at 4.6min, with maximal response detected at 325mV. HPLC analysis was performed as described above, except for the injection volume being 20μl. Vanillic acid standard was dissolved in DMSO and diluted to the range of levels detected for experimental samples (Sigma, St. Louis, MO). Activity was expressed as picogram of vanillic acid formed per minute per mg protein. Data were analyzed by two-way ANOVA and presented as mean ± SEM; asterisks indicate significance compared with control at *=P≤0.05, **=P≤0.01, ***=P≤0.001 (Bonferroni's post-hoc t-test).

4.4 Dopamine, DOPAC and HV A Level Analysis

Aliquots from each tissue homogenate (800μl) were deproteinized by the addition of 200μl of 2M $HClO_4$ (Sigma, St. Louis, MO) and sonicated on ice using a tip sonicator to liberate bound catecholamines and metabolites. Samples were then centrifuged for 10 minutes at 13,000rpm (4°C) and supernatants were passed through 0.2μm syringe-driven filters (VWR International, Bridgeport, NJ) and stored at -80°C until chromatographic analysis. Pellets from each spin were collected, resuspended in 0.5 NaOH to neutralize, sonicated, respun, and supernatants collected for a Lowry protein assay. Standard solutions for HVA, Dopamine, and DOPAC were prepared in the ranges of detected tissue metabolites (Sigma, St. Louis, MO). Metabolites were expressed as picogram of the compound of interest per mg

protein injected into the HPLC system. Samples were injected at a volume of 50μl using an autosampler with a cooled tray system (ESA Model 542 autosampler). A two-pump solvent delivery apparatus was utilized (ESA 582 module), with compound separation achieved using ESA column 70-0636 (ESA, Chelmsford, MA). Fractionated samples were subsequently detected using an in-line electrochemical detection system, utilizing an 8-channel array with potentials set to 400, 325, 250, 175, 100, 25, -50, and -125mV (ESA Coularray 5600A detector). ESA MD-TM mobile phase was delivered at a rate of 0.9ml/min for the duration of the sample runs. Data was analyzed using the ESA Coularray software package. Dopamine, HVA, and DOPAC peaks were detected at 3.33, 5.65 and 2.73 minutes, with maximal responses found at channels set to 25, 250 and 100mV, respectively. Values for each peak were then normalized to total protein amount and data presented as ng of catecholamine per mg protein. Analyses were performed using three each of three and nine month old *Cln3*$^{-/-}$ and wild type (129/SvJ/SVJ) mice, with brains microdissected into cerebellum, cortex, and striatum. Homogenates were subdivided into five separate samples prior to processing, each an n=15 for each test group. Data were analyzed by two-way ANOVA and presented as mean ± SEM; asterisks indicate significance compared with control at *=P≤0.05, **=P≤0.01, ***=P≤0.001 (Bonferroni's post-hoc t-test).

4.5 Carbonyl Dot Blot

Protein samples were vacuum dot blotted (Gibco Life Technologies, Rockville, MD) onto PVDF which had been activated in 100% methanol and transfer buffer (25 mM Tris, 200 mM glycine, and 20% methanol) in the amount of 25 and 50 μg. Samples were collected, rinsed in water and incubated for 15 minutes in Sypro Ruby Red (Molecular Probes, Eugene, OR). Following washing in water, images were captured under UV light and used for densitometry of total protein amounts. Membranes were then incubated in 2N HCl with DNPH (0.1mg/ml) for 5 minutes, washed in 2N HCl and then washed seven times in 100% methanol for 5 minutes each. Following one wash in PBST (10 mM sodium phosphate, pH 7.2, 0.9% NaCl, 0.1% Tween 20), membranes were incubated for one hour in blocking buffer (PBST with 5% nonfat dried milk), washed three times in PBST, and then carbonyl formation was detected by incubation with anti-DNP diluted in blocking buffer for two hours (Chemicon, Temecula, CA). Blots were then washed in PBST and incubated in secondary antibody (Goat anti-rabbit-HRP, Chemicon, Temecula, CA) for 1 hour at room temperature. Densitometry of immunoblots was performed to determine the average pixel value over dot minus background and normalizing to total protein loaded per spot based on Sypro Ruby Red staining. Data were analyzed and presented as mean ± SEM; asterisks indicate significance compared with control at p≤0.05 (Student's t-test).

4.6 Measurements of Substantia nigra volume and cell counts

Unbiased Cavalieri estimates of the volume of the substantia nigra pars compact and pars reticulata were made from six month male 129/SvJ and *Cln3*$^{-/-}$ mice (n=4/test group) as described previously, with no prior knowledge of genotype (Bible et al., 2004; Pontikis et al., 2004). The boundaries of nuclei were defined by reference to landmarks in Paxinos and Franklin (Paxinos and Franklin, 2001). Regional volumes were expressed in μm^3 and the mean volume of each region calculated for control and homozygous *Cln3*$^{-/-}$ mice. Unbiased optical estimates of neuronal survival within the pars compacta and pars reticulata were

calculated using *StereoInvestigator* software (Microbrightfield Inc., Williston, VT) to obtain unbiased optical fractionator estimates of cell numbers from either Nissl stained sections at six months of age or cell type specific immuno-stained sections at three, six, or nine months of age. For immunohistochemical analysis, brain samples were collected and sectioned as outlined above. Free floating sections were processed using standard immunohistochemical techniques as described previously (Bible et al., 2004). Antibodies used were tyrosine hydroxylase (Chemicon, Temecula, CA) and parvalbumin (Swant Inc, Bellinzona, Switzerland). Unbiased optical fractionator cell counts were performed as described previously (Bible et al., 2004; Pontikis et al., 2004), with a random starting section chosen, followed by every second stained section thereafter. Only neurons with a clearly identifiable nucleus were sampled and all counts were carried out using a 100× oil objective (NA 1.4). Data were analyzed and presented as mean ± SEM; asterisks indicate significance compared with control at $p \leq 0.05$ (Student's t-test). The mean co-efficient of error (CE) for all individual optical fractionator and nucleator estimates was calculated according to the method of Gundersen and Jensen and was less than 0.08 in all these analyses (Gundersen and Jensen, 1987).

Supplementary Material

Refer to Web version on PubMed Central for supplementary material.

Acknowledgments

The authors wish to thank Charlie Pontikis for assistance in analysis of stereology data; and Timothy Curran, Andrew Serour, and Sarah Leistman for technical assistance. This work was funded in part by National Institutes of Health (NIH) NS40580 and NS44310 (DAP), NS41930 (JDC), student fellowships NIH T32 MH065181 (JMW), NIH T32 ES07026 (DWS), Batten Disease Support and Research Association (JMW, JWB), The Luke and Rachel Foundation (DMR) and NIH R25 GMO64113 (YME).

Bibliography

Aberg L, Liewendahl K, Nikkinen P, Autti T, Rinne JO, Santavuori P. Decreased striatal dopamine transporter density in JNCL patients with parkinsonian symptoms. Neurology. 2000; 54:1069–1074. [PubMed: 10720276]

Aberg LE, Rinne JO, Rajantie I, Santavuori P. A favorable response to antiparkinsonian treatment in juvenile neuronal ceroid lipofuscinosis. Neurology. 2001; 56:1236–1239. [PubMed: 11342698]

Axelrod J, Tomchick R. Enzymatic O-methylation of epinephrine and other catechols. J Biol Chem. 1958; 233:702–705. [PubMed: 13575440]

Barisic N, Logan P, Pikija S, Skarpa D, Blau N. R208× mutation in CLN2 gene associated with reduced cerebrospinal fluid pterins in a girl with classic late infantile neuronal ceroid lipofuscinosis. Croat Med J. 2003; 44:489–493. [PubMed: 12950156]

Benedict JW, Sommers CA, Pearce DA. Progressive oxidative damage in the the CNS of a Murine Model of Juvenile Batten Disease. Journal of Neuroscience Research. 2007 In press.

Bible E, Gupta P, Hofmann SL, Cooper JD. Regional and cellular neuropathology in the palmitoyl protein thioesterase-1 null mutant mouse model of infantile neuronal ceroid lipofuscinosis. Neurobiol Dis. 2004; 16:346–359. [PubMed: 15193291]

Boudikova B, Szumlanski C, Maidak B, Weinshilboum R. Human liver catechol-O-methyltransferase pharmacogenetics. Clin Pharmacol Ther. 1990; 48:381–389. [PubMed: 2225698]

Brooks AI, Chattopadhyay S, Mitchison HM, Nussbaum RL, Pearce DA. Functional categorization of gene expression changes in the cerebellum of a Cln3-knockout mouse model for Batten disease. Mol Genet Metab. 2003; 78:17–30. [PubMed: 12559844]

Dalle-Donne I, Giustarini D, Colombo R, Rossi R, Milzani A. Protein carbonylation in human diseases. Trends Mol Med. 2003a; 9:169–176. [PubMed: 12727143]

Dalle-Donne I, Rossi R, Giustarini D, Milzani A, Colombo R. Protein carbonyl groups as biomarkers of oxidative stress. Clin Chim Acta. 2003b; 329:23–38. [PubMed: 12589963]

Ellingson T, Duddempudi S, Greenberg BD, Hooper D, Eisenhofer G. Determination of differential activities of soluble and membrane-bound catechol-O-methyltransferase in tissues and erythrocytes. J Chromatogr B Biomed Sci Appl. 1999; 729:347–353. [PubMed: 10410961]

Elshatory Y, Brooks AI, Chattopadhyay S, Curran TM, Gupta P, Ramalingam V, Hofmann SL, Pearce DA. Early changes in gene expression in two models of Batten disease. FEBS Lett. 2003; 538:207–212. [PubMed: 12633880]

Fan JB, Zhang CS, Gu NF, Li XW, Sun WW, Wang HY, Feng GY, St Clair D, He L. Catechol-O-methyltransferase gene Val/Met functional polymorphism and risk of schizophrenia: a large-scale association study plus meta-analysis. Biol Psychiatry. 2005; 57:139–144. [PubMed: 15652872]

Fossale E, Wolf P, Espinola JA, Lubicz-Nawrocka T, Teed AM, Gao H, Rigamonti D, Cattaneo E, MacDonald ME, Cotman SL. Membrane trafficking and mitochondrial abnormalities precede subunit c deposition in a cerebellar cell model of juvenile neuronal ceroid lipofuscinosis. BMC Neurosci. 2004; 5:57. [PubMed: 15588329]

Galderisi S, Maj M, Kirkpatrick B, Piccardi P, Mucci A, Invernizzi G, Rossi A, Pini S, Vita A, Cassano P, Stratta P, Severino G, Del Zompo M. Catechol-O-Methyltransferase ValMet Polymorphism in Schizophrenia: Associations with Cognitive and Motor Impairment. Neuropsychobiology. 2005; 52:83–89. [PubMed: 16037677]

Glaser CB, Yamin G, Uversky VN, Fink AL. Methionine oxidation, alpha-synuclein and Parkinson's disease. Biochim Biophys Acta. 2005; 1703:157–169. [PubMed: 15680224]

Guldberg HC, Marsden CA. Catechol-O-methyl transferase: pharmacological aspects and physiological role. Pharmacol Rev. 1975; 27:135–206. [PubMed: 1103160]

Gundersen HJ, Jensen EB. The efficiency of systematic stereology and its prediction. J Microsc. 1987; 147:229–263. [PubMed: 3430576]

Hofman, I.; Kohlschutter, A.; Santavuori, P.; Gottlob, I.; Goebel, HH.; Lake, BD.; Schutgens, RBH.; Greene, ND.; Leung, KY.; Mitchison, HM.; Munroe, PB.; Taschner, PE. The neuronal ceroid lipofuscinses (Batten disease). Amsterdam, The Netherlands: IOS Press; 1999.

Holton KL, Loder MK, Melikian HE. Nonclassical, distinct endocytic signals dictate constitutive and PKC-regulated neurotransmitter transporter internalization. Nat Neurosci. 2005

Horowitz A, Shifman S, Rivlin N, Pisante A, Darvasi A. A survey of the 22q11 microdeletion in a large cohort of schizophrenia patients. Schizophr Res. 2005; 73:263–267. [PubMed: 15653270]

Hsu M, Srinivas B, Kumar J, Subramanian R, Andersen J. Glutathione depletion resulting in selective mitochondrial complex I inhibition in dopaminergic cells is via an NO-mediated pathway not involving peroxynitrite: implications for Parkinson's disease. J Neurochem. 2005; 92:1091–1103. [PubMed: 15715660]

Kandel, ER.; Schwartz, JH.; Jessell, TM. Principles of Neural Science. 4th. New York, NY: McGraw-Hill; 2000.

Kielar C, Maddox L, Bible E, Pontikis CC, Macauley SL, Griffey MA, Wong M, Sands MS, Cooper JD. Successive neuron loss in the thalamus and cortex in a mouse model of infantile neuronal ceroid lipofuscinosis. Neurobiol Dis. 2007; 25:150–162. [PubMed: 17046272]

Koike H, Arguello PA, Kvajo M, Karayiorgou M, Gogos JA. Disc1 is mutated in the 129S6/SvEv strain and modulates working memory in mice. Proc Natl Acad Sci U S A. 2006; 103:3693–3697. [PubMed: 16484369]

Kovacs AD, Weimer JM, Pearce DA. Selectively increased sensitivity of cerebellar granule cells to AMPA receptor-mediated excitotoxicity in a mouse model of Batten disease. Neurobiol Dis. 2006

Lin WC, Tsai PS, Huang CJ. Catecholamines' enhancement of inducible nitric oxide synthase-induced nitric oxide biosynthesis involves CAT-1 and CAT-2A. Anesth Analg. 2005; 101:226–232. table of contents. [PubMed: 15976236]

Luiro K, Yliannala K, Ahtiainen L, Maunu H, Jarvela I, Kyttala A, Jalanko A. Interconnections of CLN3, Hook1 and Rab proteins link Batten disease to defects in the endocytic pathway. Hum Mol Genet. 2004; 13:3017–3027. [PubMed: 15471887]

Lundstrom K, Salminen M, Jalanko A, Savolainen R, Ulmanen I. Cloning and characterization of human placental catechol-O-methyltransferase cDNA. DNA Cell Biol. 1991; 10:181–189. [PubMed: 1707278]

Malherbe P, Bertocci B, Caspers P, Zurcher G, Da Prada M. Expression of functional membrane-bound and soluble catechol-O-methyltransferase in Escherichia coli and a mammalian cell line. J Neurochem. 1992; 58:1782–1789. [PubMed: 1560233]

Mitchison HM, Bernard DJ, Greene ND, Cooper JD, Junaid MA, Pullarkat RK, de Vos N, Breuning MH, Owens JW, Mobley WC, Gardiner RM, Lake BD, Taschner PE, Nussbaum RL. Targeted disruption of the Cln3 gene provides a mouse model for Batten disease. The Batten Mouse Model Consortium. Neurobiol Dis. 1999; 6:321–334. [PubMed: 10527801]

Paxinos, G.; Franklin, KBJ. The Mouse Brain in Stereological Coordinates. 2nd. San Diego, California: Academic Press; 2001.

Pihlavisto P, Reenila I. Separation methods for catechol O-methyltransferase activity assay: physiological and pathophysiological relevance. J Chromatogr B Analyt Technol Biomed Life Sci. 2002; 781:359–372.

Pontikis CC, Cotman SL, Macdonald ME, Cooper JD. Thalamocortical neuron loss and localized astrocytosis in the Cln3(Deltaex7/8) knock-in mouse model of Batten disease. Neurobiol Dis. 2005

Pontikis CC, Cella CV, Parihar N, Lim MJ, Chakrabarti S, Mitchison HM, Mobley WC, Rezaie P, Pearce DA, Cooper JD. Late onset neurodegeneration in the Cln3-/- mouse model of juvenile neuronal ceroid lipofuscinosis is preceded by low level glial activation. Brain Res. 2004; 1023:231–242. [PubMed: 15374749]

Porzgen P, Bonisch H, Bruss M. Molecular cloning and organization of the coding region of the human norepinephrine transporter gene. Biochem Biophys Res Commun. 1995; 215:1145–1150. [PubMed: 7488042]

Ramirez-Montealegre D, Pearce DA. Defective lysosomal arginine transport in juvenile Batten disease. Hum Mol Genet. 2005; 14:3759–3773. [PubMed: 16251196]

Reenila I, Tuomainen P, Mannisto PT. Improved assay of reaction products to quantitate catechol-O-methyltransferase activity by high-performance liquid chromatography with electrochemical detection. J Chromatogr B Biomed Appl. 1995; 663:137–142. [PubMed: 7704200]

Reenila I, Tuomainen P, Soinila S, Mannisto PT. Increase of catechol-O-methyltransferase activity in rat brain microglia after intrastriatal infusion of fluorocitrate, a glial toxin. Neurosci Lett. 1997; 230:155–158. [PubMed: 9272684]

Rinne JO, Ruottinen HM, Nagren K, Aberg LE, Santavuori P. Positron emission tomography shows reduced striatal dopamine D1 but not D2 receptors in juvenile neuronal ceroid lipofuscinosis. Neuropediatrics. 2002; 33:138–141. [PubMed: 12200743]

Rivett AJ, Francis A, Roth JA. Localization of membrane-bound catechol-O-methyltransferase. J Neurochem. 1983a; 40:1494–1496. [PubMed: 6834074]

Rivett AJ, Francis A, Roth JA. Distinct cellular localization of membrane-bound and soluble forms of catechol-O-methyltransferase in brain. J Neurochem. 1983b; 40:215–219. [PubMed: 6848660]

Ruottinen HM, Rinne JO, Haaparanta M, Solin O, Bergman J, Oikonen VJ, Jarvela I, Santavuori P. [18F]fluorodopa PET shows striatal dopaminergic dysfunction in juvenile neuronal ceroid lipofuscinosis. J Neurol Neurosurg Psychiatry. 1997; 62:622–625. [PubMed: 9219750]

Salminen M, Lundstrom K, Tilgmann C, Savolainen R, Kalkkinen N, Ulmanen I. Molecular cloning and characterization of rat liver catechol-O-methyltransferase. Gene. 1990; 93:241–247. [PubMed: 2227437]

Sappington RM, Pearce DA, Calkins DJ. Optic nerve degeneration in a murine model of juvenile ceroid lipofuscinosis. Invest Ophthalmol Vis Sci. 2003; 44:3725–3731. [PubMed: 12939285]

Seigel GM, Lotery A, Kummer A, Bernard DJ, Greene ND, Turmaine M, Derksen T, Nussbaum RL, Davidson B, Wagner J, Mitchison HM. Retinal pathology and function in a Cln3 knockout mouse model of juvenile Neuronal Ceroid Lipofuscinosis (batten disease). Mol Cell Neurosci. 2002; 19:515–527. [PubMed: 11988019]

Tai CH, Wu RM. Catechol-O-methyltransferase and Parkinson's disease. Acta Med Okayama. 2002; 56:1–6. [PubMed: 11873938]

Torres GE, Gainetdinov RR, Caron MG. Plasma membrane monoamine transporters: structure, regulation and function. Nat Rev Neurosci. 2003; 4:13–25. [PubMed: 12511858]

Weimer JM, Chattopadhyay S, Custer AW, Pearce DA. Elevation of Hook1 in a disease model of Batten disease does not affect a novel interaction between Ankyrin G and Hook1. Biochem Biophys Res Commun. 2005; 330:1176–1181. [PubMed: 15823567]

Weinshilboum R, Raymond F. Variations in catechol-O-methyltransferase activity in inbred strains of rats. Neuropharmacology. 1977; 16:703–706. [PubMed: 304191]

Winqvist R, Lundstrom K, Salminen M, Laatikainen M, Ulmanen I. The human catechol-O-methyltransferase (COMT) gene maps to band q11.2 of chromosome 22 and shows a frequent RFLP with BglI. Cytogenet Cell Genet. 1992; 59:253–257. [PubMed: 1347500]

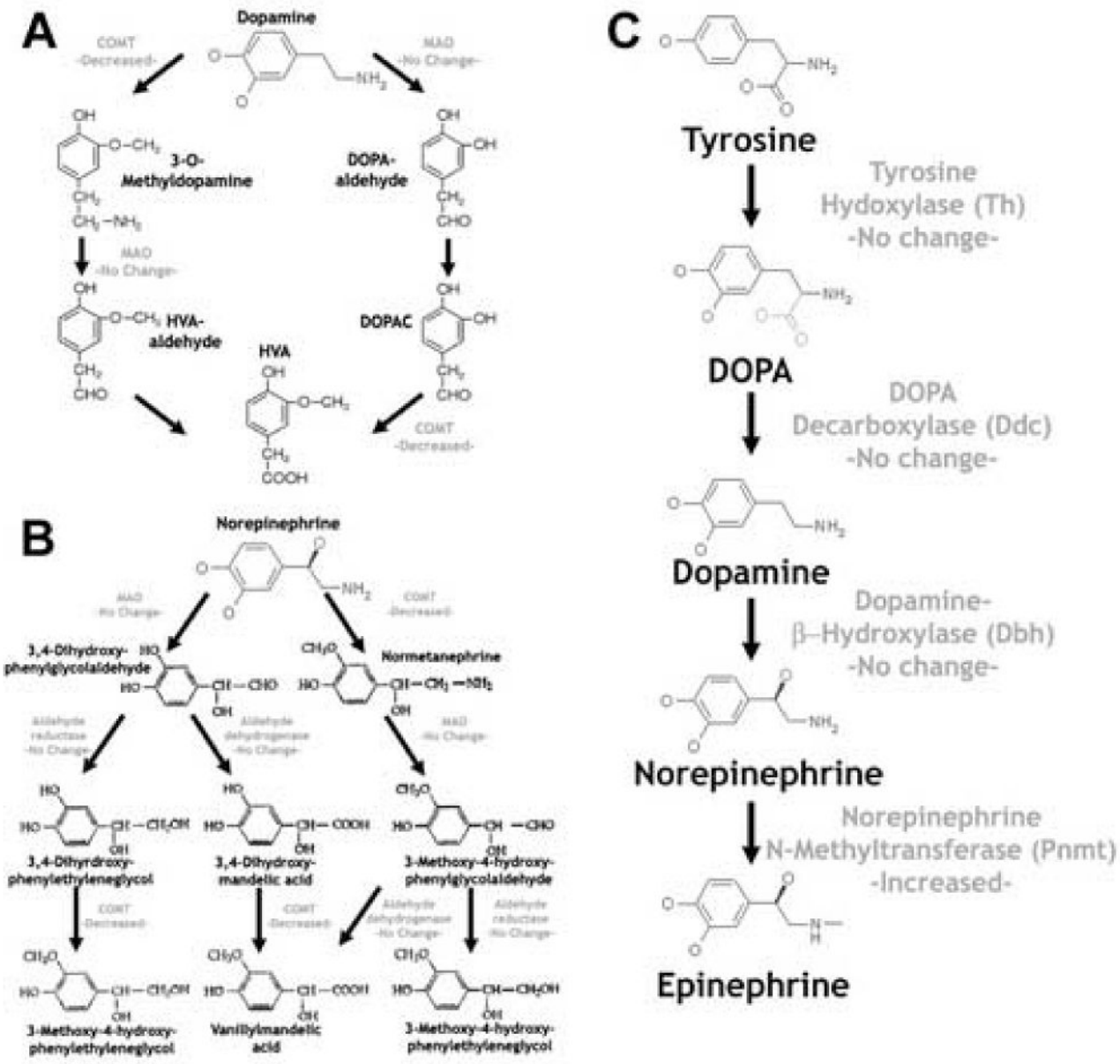

Figure 1. Deficits genes involved in catecholamine metabolism is restricted to a decreased in COMT in the Cln3$^{-/-}$ mice

Evaluation of several published microarray data sets performed on the *Cln3*$^{-/-}$mice showed a selective down regulation in the expression of *Comt* (3.56 fold decrease, 10-week whole brain microarray) with a sparing of all other enzymes involved in catecholamine catabolism (Dopamine, **A** & Norepinephrine, **B**) (Brooks et al., 2003; Elshatory et al., 2003). Synthesis of catecholamine is achieved through conversion of tyrosine to DOPA, followed by the subsequent selective conversion to dopamine, norepinephrine, and epinephrine. Of the enzymes involved in the production of catecholamines, specifically tyrosine hydroxylase, DOPA decarboxylase, dopamine β-hydroxylase, and norephinephrine N-methyltransferase (*Pnmt*) none were altered in the *Cln3*$^{-/-}$ mice aside from a slight, yet significant, decrease in

the level of *Pnmt*, suggesting disruption in the enzyme involved in conversion of norepinephrine to epinephrine [less than 1.5 fold change ($p \leq 0.05$, Student's t-test), 10-week whole brain microarray (Brooks et al., 2003)] (**C**).

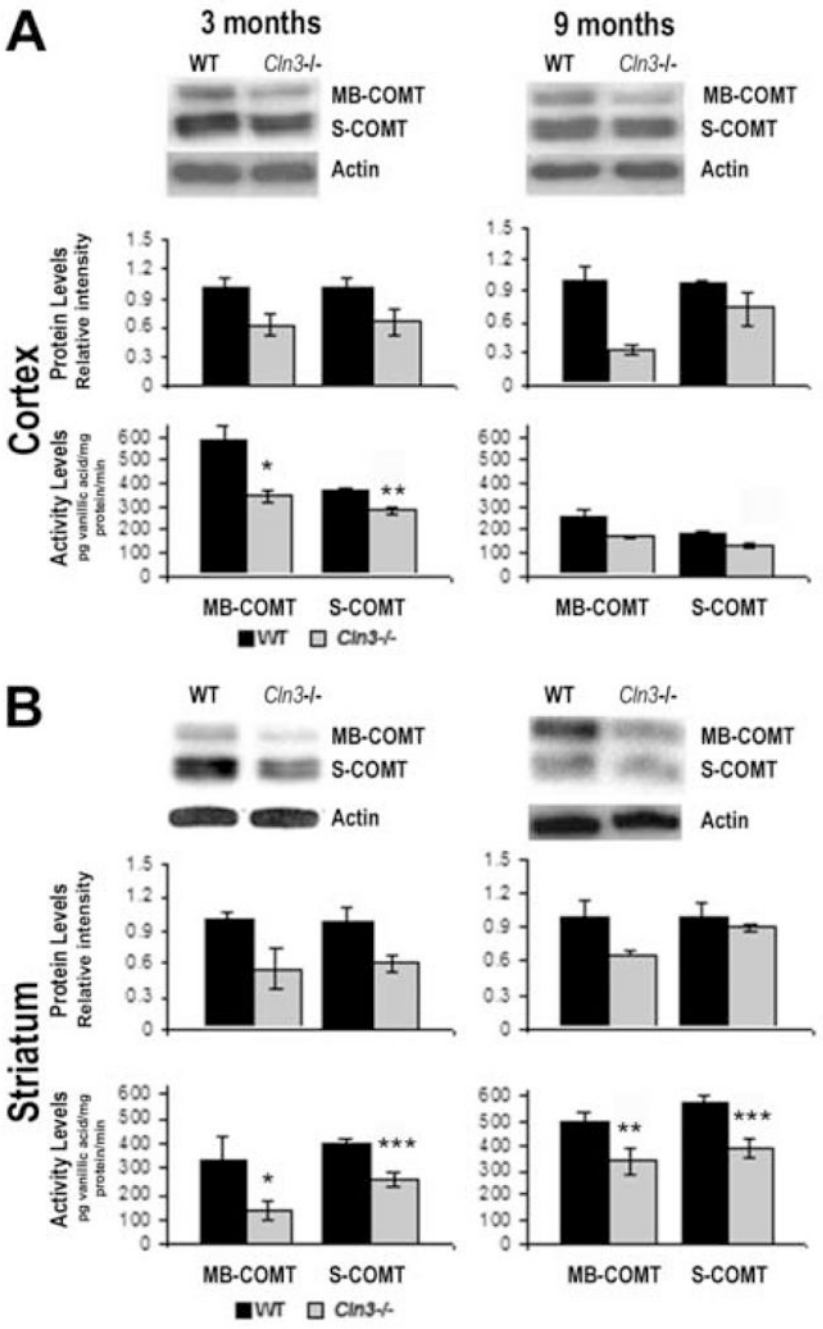

Figure 2. Decreased COMT protein and activity levels in 3 and 9 month Cln3$^{-/-}$ mice cortex and striatum

Immunoblotting for catechol-O-methyl transferase (COMT) revealed changes in both the membrane bound (MB) and soluble (S) form of the protein in brain samples from *Cln3*$^{-/-}$mice compared to wild-type mice. Samples were prepared from cortex (**A**) and striatum (**B**) of both three and nine month old male mice. Top panels show representative level of COMT from the indicated samples (13% SDS-PAGE) while the lower band shows actin immunoblotting. Histograms in the lower panel depict relative levels of MB-COMT

and S-COMT in wild-type and *Cln3*$^{-/-}$ mice. Densitometry of MB-COMT and S-COMT bands were standardized to actin densities, with background subtraction being performed for both COMT and actin bands. (Mean relative intensity ± SEM). O-methylating activity of COMT was assayed by enriching for the S- or MB-COMT fractions by centrifugation at 100,000×g (confirmed by western blot), mixing samples with the co-factor S-adenosylmethionine (SAM), followed by reaction with dihydroxybenzoic acid. O-methylation of dihydroxybenzoic acid (DHBAc) to vanillic acid was assessed after 60 minute incubation times by HPLC (**A, B, lower row**). Samples were prepared from cortex (**A**) and striatum (**B**) of both three (left column) and nine month (right column) old male *Cln3*$^{-/-}$ and 129/SvJ wild-type mice. Decreases in the activity of S-COMT were seen at both time points in cortex and striatum (**A, B, lower row**). Significant decreases in activity of the MB-COMT were seen only at nine months in the striatum (**B**) Activity is represented as mean pg vanillic acid/mg protein/minute ± SEM; *P≤0.05, ** P≤0.01, *** P≤0.001 (2-way ANOVA).

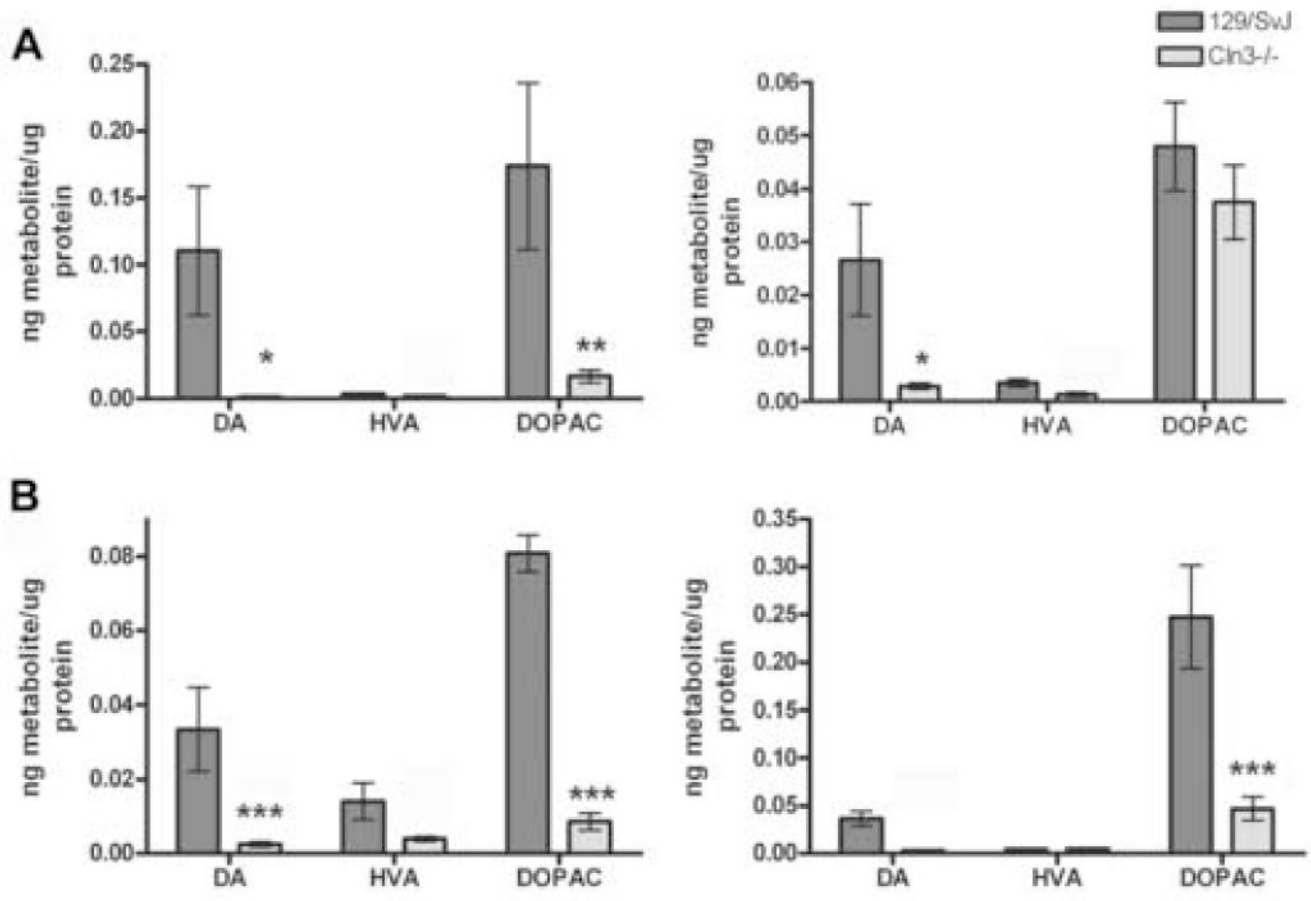

Figure 3. Alterations in level of Dopamine, DOPAC, and H VA in midbrain and cortex wild-type and Cln3$^{-/-}$ mice

Deproteinized homogenates were sonicated and catecholamine metabolites were fractionated on an ESA column (70-0636). Dopamine, HVA and DOPAC came off at 3.33, 5.65, and 2.73 minutes, and showed maximum responses at channels set to 25, 250 and 100mV, respectively. The levels of dopamine, HVA, and DOPAC were assayed three and nine month old *Cln3-/-* and 129/SvJ wild-type mice in cortex and midbrain and presented as level of metabolite in ng normalized to the total amount of protein in μg. This analysis revealed global disruption in the levels of these metabolites in *Cln3-/-* mice. In both the cerebral cortex (**A**) and the striatum (**B**) there was a significant decrease in the levels of dopamine and DOPAC, although HVA levels remained unaffected. Data are presented as mean ng metabolite/μg total protein ± SEM, *P≤0.05, ** P≤0.01, *** P≤0.001 (2-way ANOVA).

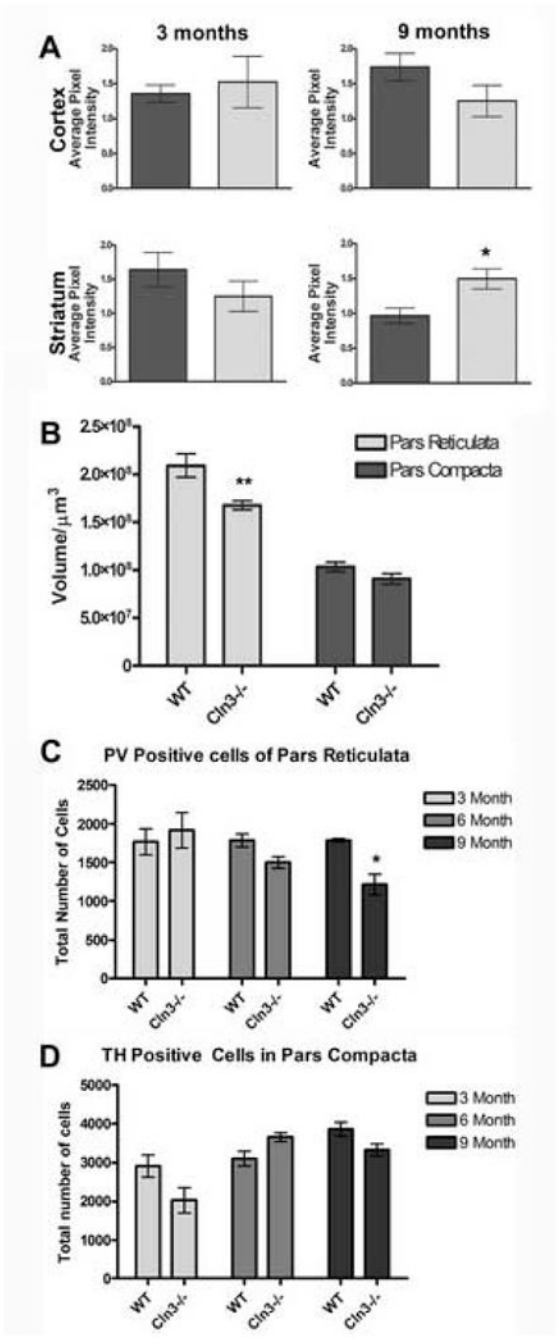

Figure 4. Elevated oxidative striatal stress and cellular atrophy in the substantia nigra pars reticulata of Cln3$^{-/-}$ mice

Proteins from three and nine month old male *Cln3*$^{-/-}$ and 129/SvJ cortex (**A, upper row**) and striatum (**A, lower row**) were dot blotted onto PVDF and carbonyls were derivativitzed with DNPH to form a stable product that was detected by immunoblotting. This revealed an increase in the level of oxidative stress at nine months of age in the striatum of *Cln3*$^{-/-}$ mice (**A, lower right panel**). Histograms depict densitometry of derivatized carbonyls standardized to total protein, determined by staining of the PVDF with Sypro Ruby Red

(Mean relative intensity ± SEM). Unbiased Cavalieri estimates of regional volume were measured on Nissl stained brain sections. Regional volumes were expressed in μm^3 and the mean volume of each region calculated for control and homozygous *Cln3*$^{-/-}$ mice. There was a significant regional atrophy was seen in *Cln3*$^{-/-}$ vs. 129/SvJ (+/+) at six months of age within the substantia nigra pars reticulata (SN-pr) (**B, left panel**), although no difference was observed in the volume of the substantia nigra pars compacta (**B, right panel**). This cell loss was specific to the parvalbumin positive cells of the pars reticulata and was progressive as the animals aged. Optical fractionator cell counts of the substantia nigra pars reticulata and pars compacta were performed to determine absolute numbers of cells within each region. To distinguish cells types, cells of the pars reticulata were immuno-labeled with parvalbumin (PV) and the cells of the pars compacta were labeled with tyrosine hydroxylase at three, six, and nine months of age. A significant decrease was seen in the number of PV positive pars reticulata cells, progressing to near 35% cell loss by nine months of age (129/SvJ: 1788±21.3, *Cln3*$^{-/-}$: 1214±135.87) although no change was seen at the early time points (3 month: 129/SvJ: 1766±166.89, *Cln3*$^{-/-}$: 1916±228.27; 6 month: 129/SvJ: 1785±87.79, *Cln3*$^{-/-}$: 1501±72.68) (**C**). No decrease within the pars compacta was noted at any of the time points (3 month: 129/SvJ: 2906±287.23, *Cln3*$^{-/-}$: 2023±329.48; 6 month: 129/SvJ: 3100±193.69, *Cln3*$^{-/-}$: 3650±109.83; 9 month: 129/SvJ: 3859±74.71, *Cln3*$^{-/-}$: 3324±153.05) (**D**). Data are presented as mean ± SEM, *$p \leq 0.05$, ** $p \leq 0.01$ (Student's t-test).

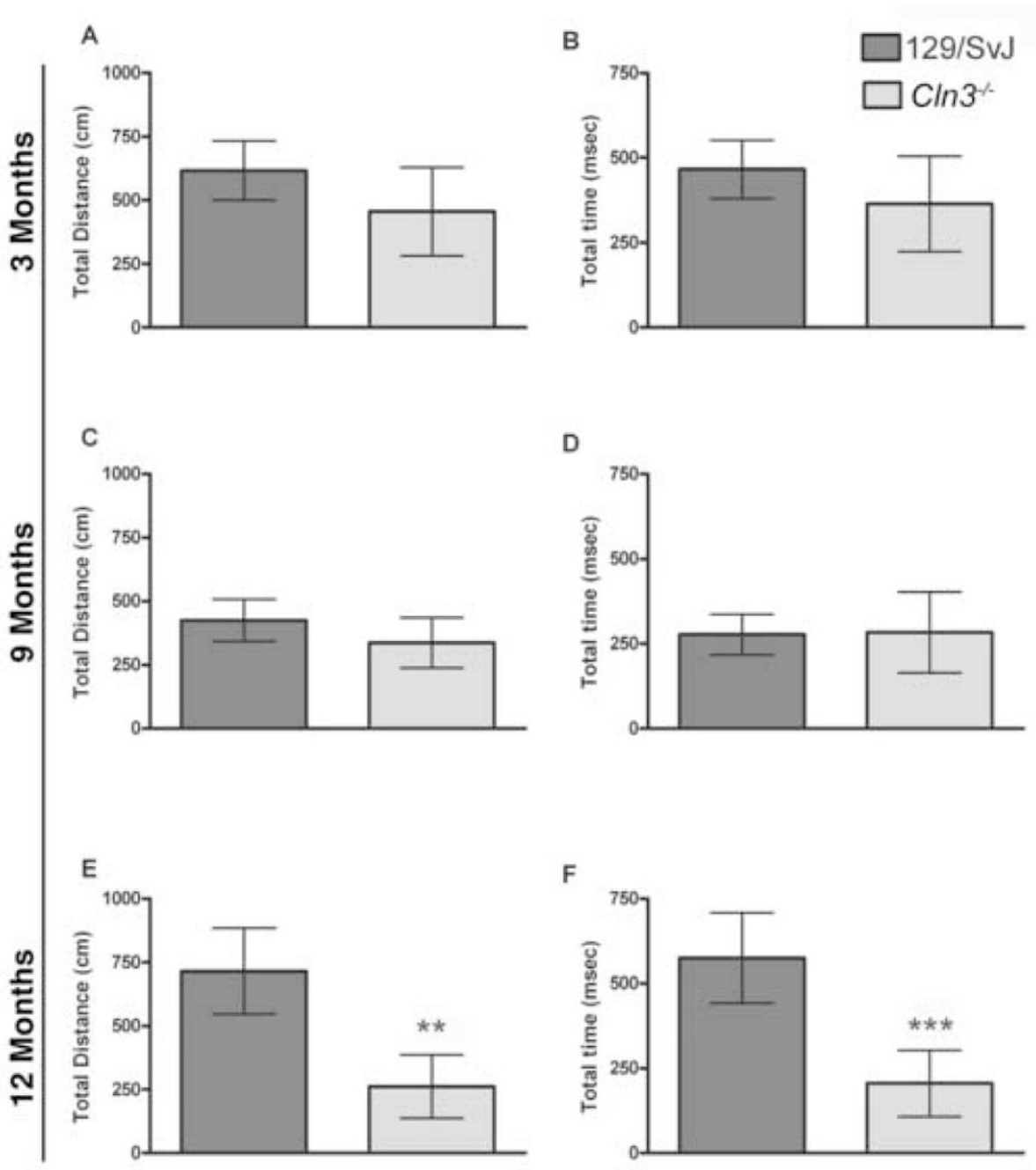

Figure 5. Degenerative changes in motor activity of Cln3$^{-/-}$ mice

Locomotor testing was performed on 129/SvJ and *Cln3*$^{-/-}$ mice at three different time points in an open field activity chamber. Animals were habituated for two days for 30 minutes followed by testing trial of 30 minutes. Separate groups of mice were tested at three, nine, and twelve months of age. The total distance each animal traveled (**A, C, E**) and the amount of time spent moving (**B, D, F**) was calculated. No differences in total distance traveled or time spent ambulating was detected at three or nine months of age. By twelve months of age, there was a significant decrease in distance traveled and amount of time spent

ambulating in *Cln3*$^{-/-}$ mice (**E-F**). Mean time or distance traveled ± SEM, two way ANOVA, $F(1,23)=2.421$, $P=0.004$ (time) and ($F(1,23)=2.560$, $P=0.001$ (distance).

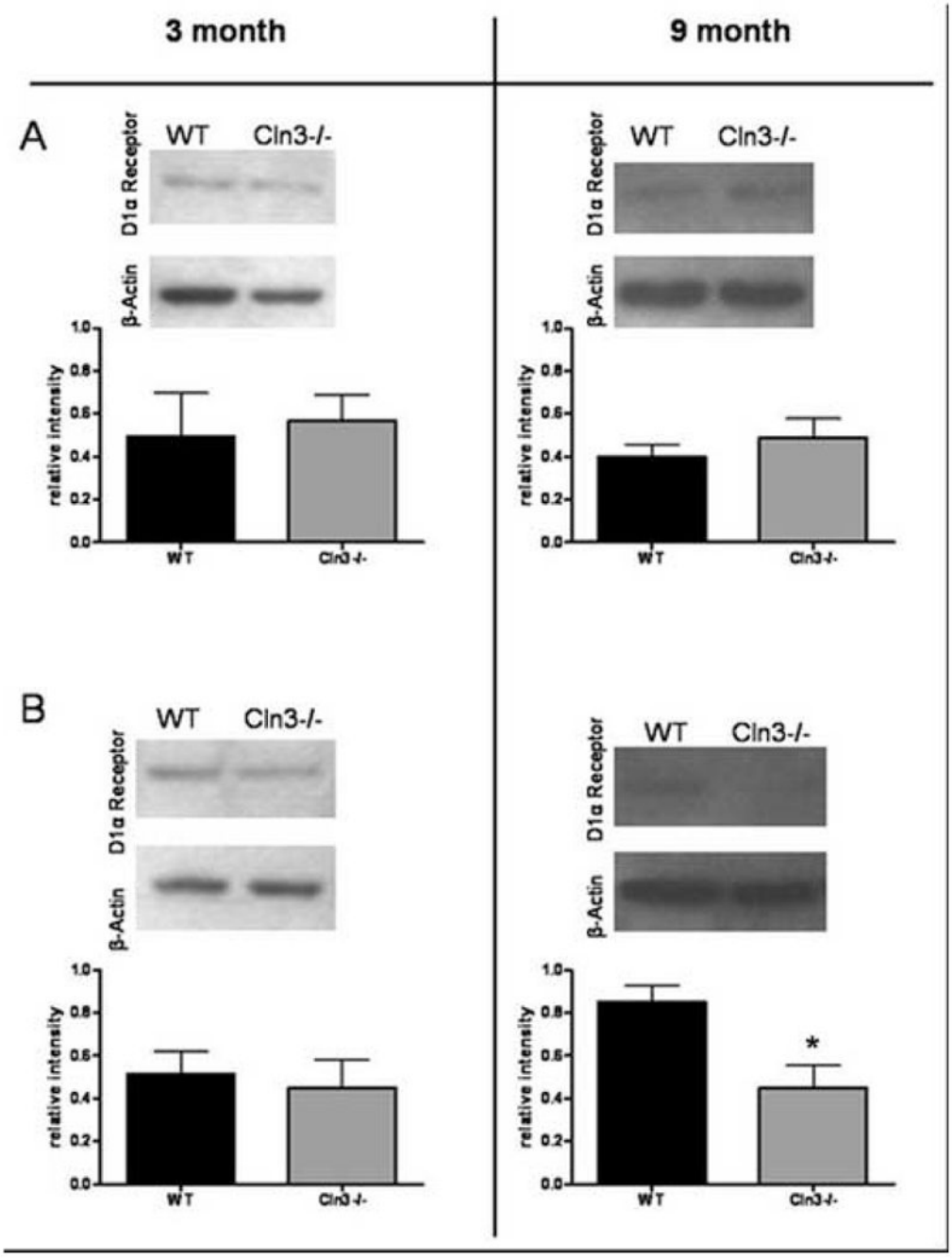

Figure 6. Decreased D1α receptor expression at nine month Cln3$^{-/-}$ mice striatum

Immunoblotting for the dopamine 1α (D1α) receptor revealed a decrease in the expression level of the protein in striatum brain samples from nine month old *Cln3*$^{-/-}$ mice compared to 129/SvJ wild-type mice. Samples were prepared from cortex (**A**) and striatum (**B**) of both three and nine month old male mice. Top panels show level of D1α receptor from the indicated samples while the lower band shows actin immunoblotting. Histograms in the lower panel depict relative levels of D1α receptor in wild-type and *Cln3*$^{-/-}$ mice. Densitometry of D1α receptor bands were standardized to actin densities, with background

subtraction being performed for both receptor and actin bands. Data are presented as mean ± SEM, *p≤0.05 (Student's t-test).

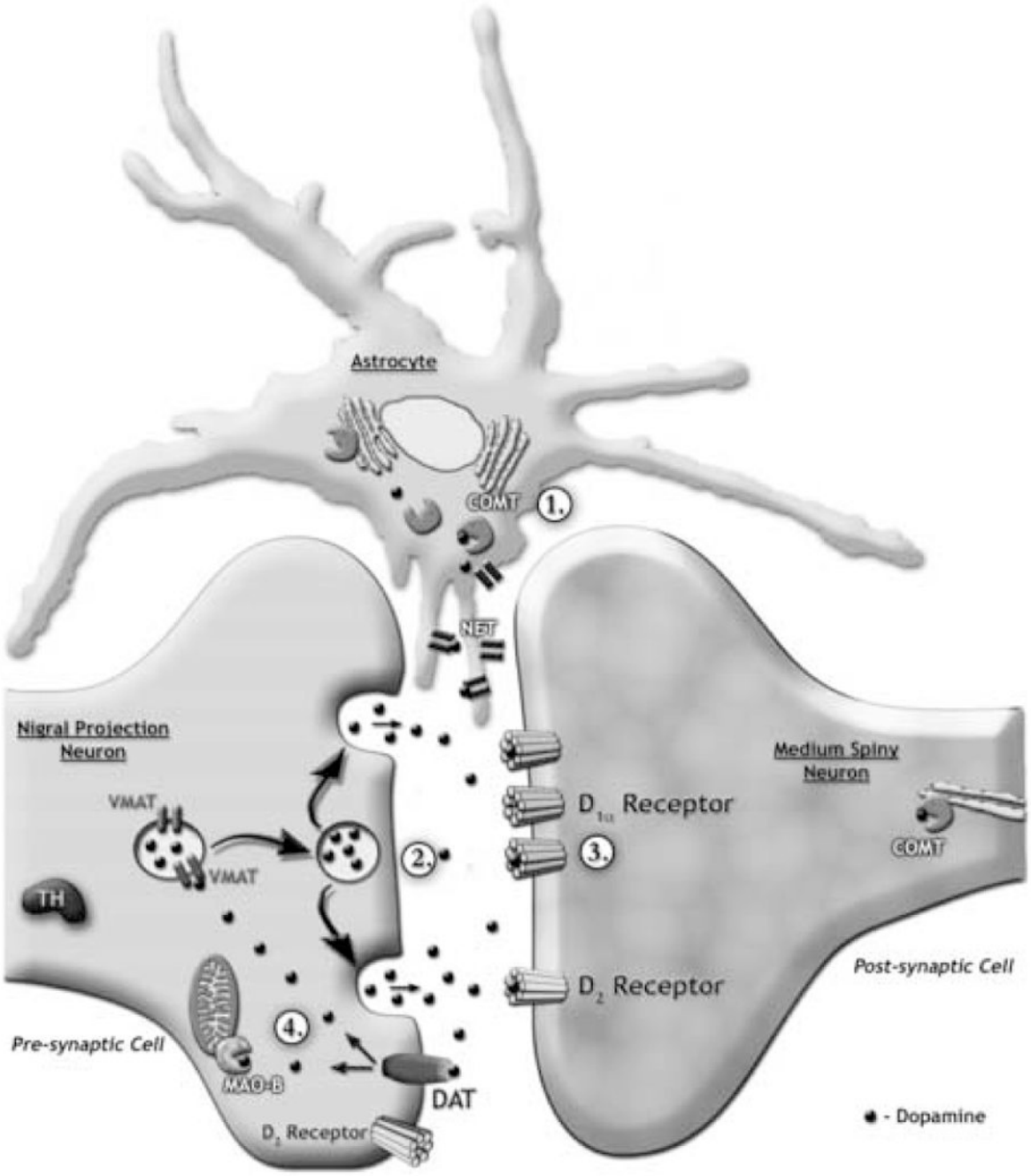

Figure 7. Summary of dopamine metabolism and handling

1. Decrease in both COMT levels and activity
2. Decrease in the metabolites dopamine and DOPAC
3. Decrease in the postsynaptic $D_{1\alpha}$ receptor
4. No difference in the expression of DAT, MAO-B, VMAT, or NET